ISSN (Online): 2091-2609
DOI Prefix: 10.3126/ijasbt

International Journal of Applied Sciences and Biotechnology (IJASBT)

Research Article

Construction of an Amperometric Pyruvate Biosensor Based on Enzyme Bound to A Nanocomposite and Its Comparison with Enzyme Nanoparticles Bound to Electrode

Mansi Malik[1], Reeti Chaudhary[1], C. S. Pundir[2*]

[1]Deenbandhu Chhotu Ram University of Science and Technology, Murthal, Sonipat, Haryana-131039
[2]Department of Biochemistry, M.D. University, Rohtak, Haryana, India

Abstract

An improved amperometric pyruvate biosensor was fabricated by immobilizing covalently commercial pyruvate oxidase (POx) from *Aerococcus* sps. onto nanocomposite of c-MWCNTs (carboxylated multi- walled carbon nanotubes), copper nanoparticles (CuNPs) and polyaniline (PANI) electrodeposited onto gold (Au) electrode. The copper nanoparticles were prepared by chemical reduction method and characterized by transmission electron microscopy (TEM), UV- visible spectroscopy and X- ray diffraction (XRD). The working electrode (POx/c-MWCNT/CuNPs/PANI/AuE was studied via scanning electron microscopy (SEM), Fourier transform infrared spectrometry (FTIR) and electrochemical impedance spectroscopy (EIS) at different stages of its construction. The biosensor showed optimum activity at a pH of 5.0 and 35°C and a linearity for pyruvate in the concentration range, 0.1 µM to 2000 µM. The analytical recovery of added pyruvate was 99.6% and 99.2%. The within and between batch coefficients of variation (CV) were 0.069% and as 0.072% respectively. There was a commendable correlation between sera pyruvate values as measured by standard spectrophotometric method and the present method. The biosensor was applied to measure sera pyruvate level and compared with that biosensor based on pyruvate oxidase nanoparticles covalently bound to Au electrode.

Keywords: Pyruvate; biosensor; pyruvate oxidase; pyruvate oxidase nanoparticles; copper nanoparticles; polyaniline, carboxylated multi-walled carbon nanotubes, serum**.**

Introduction

Pyruvate is one of the important intermediary molecule holding an important position in several metabolic processes of human body like glycolysis, tricarboxylic acid cycle, lactogenesis and other metabolic pathways (Situmorang *et al.,* 2002). Since, pyruvate is involved in different energy production pathways, its presence is widely observed in living organisms. The biosynthesis of pyruvate occurs in the cells of the human body (Akylimaz and Yorganci, 2008). Over the last 20 years, several research groups have focused research on developing a novel platform for the detection of pyruvate, as it possesses

Cite this article as:

M. Malik et al. (2019) Int. J. Appl. Sci. Biotechnol. Vol 7(2): 195-206. DOI: 10.3126/ijasbt.v7i2.24445

***Corresponding author**
C. S. Pundir,
Department of Biochemistry, M.D. University, Rohtak, Haryana, India
Email: chandraspundir@gmail.com

Peer reviewed under authority of IJASBT
© 2019 International Journal of Applied Sciences and Biotechnology

This is an open access article & it is licensed under a Creative Commons Attribution 4.0 International License (https://creativecommons.org/licenses/by/4.0/)

importance in various clinical diagnosis and bioprocesses as well as food industry. Normal level of pyruvate found in circulation inside blood lies between 40- 120 µM (Kulys *et al*., 1992). Several diseased conditions cause an elevation in these designated levels of pyruvate inside human body (Gray *et al.*, 2014). Increased levels of pyruvate have been known to display symptoms of autism (Essa *et al.*, 2013). Also, physiological and biochemical fluctuations in conditions of cardiac failure is an enticing field of research in the hemodynamics. Recent research has also shown that pyruvate holds a major position in cardiovascular infarction and heart related diseases (Akyilmaz and Yorganci, 2008). Several techniques have been described during past for the determination of pyruvate like colorimetric (Anthon and Barrett, 2000) spectrophotometric enzymic assays (Berntsson, 1955), fluorimetry (Olsen, 1971; Shapiro and Silanikove, 2011) and high performance liquid chromatography (Yoo and Pike, 1999). All these methods involved sturdy and sluggish treatment steps, displayed low precision & accuracy and were expensive, laborious to operate, time- consuming and required high amount of sample (at least 5 ml) and suffer from low reusability of the enzyme. To, overcome these pitholes, the biosensors have been devised as an alternative tangible solution (Bacri and Burstein, 1987). The cutting edge advantage of the biosensor over earlier methods are that these are simple to fabricate, portable, rapid, and exhibit the increased reusability of enzyme and also require no sample pre-treatment step. Recently, we have reviewed various pyruvate biosensors, in which pyruvate oxidase (POx) has been immobilized onto several variants (Pundir *et al.*, 2019). These reported pyruvate biosensors showed reduced storage stability, decreased sensitivity, narrow range of working concentration, inferior electrical and electrochemical response. Recently, nano-composite modified electrode possessing enhanced catalytic, magnetic, electrical, mechanical and improved physiochemical properties have been put to use to ameliorate the performance of pyruvate biosensors. Copper nanoparticles provide large surface area and enhance the conductivity of the electrode since, these are highly conducive and are known to enhance the properties of the nanocrystalline materials (Din and Rehan, 2017). Polyaniline (PANI), the most facile and economically price ranged conducting polymer cited till date, is an intrinsic morphological polymer, due to its good environmental stability and de-doping chemistry (Abdolahi *et al.*, 2012). The most desired properties for choosing c- MWCNT as a nanomaterial for biosensor, has been its low capacitance due to which it acts as an efficient coupling agent. Secondly, the large current density helps enhance carrier mobility. Thereby, c-MWCNTs are a renowned material of interest in sensors construction (Jariwala *et al*., 2013). All these chosen nanomaterials have helped to impart their stupendous activity, enhanced ability and the best fit model employed to fabricate an improved amperometric biosensor. The covalent attachment of enzyme onto composite of these nanomaterials helps to upsurge the stability, accuracy and precision of the analysis. To the best of our knowledge, no report is available on use of this nanocomposite for the fabrication of a pyruvate biosensor. Recently, we have reported an improved amperometric pyruvate biosensor based on covalent immobilization of pyruvate oxidase nanoparticles (PyOxNPs) onto Au electrode (Malik *et al*., 2019). Thereby, present report describes a novel approach for fabrication of an amperometric pyruvate biosensor by immobilizing pyruvate oxidase onto composite of c-MWCNTs/CuNPs/PANI electrodeposited Au electrode and its comparison with the biosensor fabricated by direct immobilization of POxNPs/AuE.

Materials and Methods

Materials

Pyruvate oxidase (*Aerocccus* sps; E.C. number: 1.2.3.3; 100 U/mg), cofactors like thiamine pyrophosphate (TPP), magnesium chloride ($MgCl_2$) and flavin adenine dinucleotide (FAD) from Sigma- Aldrich (St. Louis, MO, USA), 2.5 cm long gold wire (23 carat) having an uniform thickness of 2.5 mm was purchased from a nearby jeweler's shop. The chemicals used during the experimentation were of analytical grade (AR).

Apparatus Used

Potentiostat/Galvanostat (Autolab, AUT83785, Eco Chemie, The Netherlands) with an inbuilt NOVA software having a three electrode system consisting of a working electrode, silver/ silver chloride as a standard and Platinum (Pt) wire as supplementary electrode. Transmission electron microscope (TEM) (Jeol, JEM, 1011), Scanning electron microscope (SEM) (Zeiss EV040, USA), Fourier transform infrared (FTIR) spectrometer (Bruker, OPUS 6.5 Software), UV- Visible spectrophotometer (Lab India Analytical, UV 3092) were used for characterization studies. The electrochemical impedance spectroscopy (EIS) was analyzed by FRA by dipping the electrodes in 5 mM potassium ferro/ ferricyanide solution at 0.5 V between a frequency range of 0.01 Hz to 10^4 Hz.

Assay of Free POx

The assay of POx was carried out as described in (Malik *et al.*, 2019).

Preparation of Copper Nanoparticles (CuNPs)

CuNPs were prepared by the chemical reduction method (Dagar and Pundir, 2017). To begin with, 0.1 M solutions of NaOH and EDTA (10 ml each) were prepared and added to an aqueous solution of $CuSO_4$ (0.4 M; 100 ml). Thereafter, 0.3 M $NaBH_4$ (100 ml) was added to the above mixture in a drop wise manner under continuous stirring followed by heating at 60°C for 45 min. The final suspension thus, obtained was washed manually 3-times

with acetone & ethanol respectively via. centrifugation and the brown colored powder was then, vacuum dried in oven at 45°C for 20 min until, a brown coloured powder of CuNPs was procured.

Characterization of CuNPs

The CuNPs were characterized via. taking its TEM images at Indian Agricultural Research Institute, New Delhi whereas, the UV- visible spectra and XRD analysis at the Department of Biotechnology, Maharishi Dayanand University Rohtak, and Department of Physics, Deenbandhu Chhotu Ram University of Science and Technology, Murthal (Sonepat) Haryana, India respectively.

Electro- Deposition of c- MWCNTs/CuNPs/PANI Hybrid Layer

A bare gold wire (2.5 cm* 2.5 mm) was cleaned with the help of silica slurry by employing a polishing cloth to get rid of any unwanted impurities sticking on the bare gold wire. The Au wire was then splashed with DW, and dipped in ethanol for 4- 5 hours to make a-OH functionalized Au electrode. Next, it was sonicated to remove the adsorbed silica particles and then, finally washed 3- 4 times with DW. Neverthless, c- MWCNTs (2.0 mg) were suspended into a 8 ml mixture of conc. H_2SO_4 and HNO_3 (in a ratio of 3: 1) and kept for ultra-sonication for 5 hours. This resulted in a finely dispersed black colored solution. In the next step, 0.1 ml of the above ultrasonicated c- MWCNT was made to react for one hour at room temperature with an equimolar solution (0.2 M each) of 0.5 ml EDC and NHS respectively. After this, 400 µl of aniline along with 25 ml 1 M KCl was electro-polymerized onto the surface of gold electrode by running 40 cycles in a potentiostat/galvanostat (NOVA 1.4). Next, CuNPs were electrodeposited onto Au electrode in a similar manner by running polymerization cycles in a potentiostat/galvanostat between -0.1 V to 0.8V. Finally, 1 ml EDC- NHS activated c- MWCNTs suspension was appended to the above 1M KCl solution. Thereafter, all the polymerization cycles resulted in the deposition of uniform hybrid layer of nano-composites.

Immobilization of POx onto Nanocomposite Modified Electrode

POx was immobilized covalently onto c-MWCNTs/CuNPs/PANI modified gold electrode as described in Ref. (Dagar and Pundir, 2017). The EDC-NHS activated cMWCNTs/CuNPs/PANI / Au electrode was immersed into 3 ml solution of POx (0.5 U/ ml) at 4°C. After incubating for 24 hours, the modified AuE was washed 3- 4 times with sodium phosphate buffer (SPB buffer, pH- 7.0). This washing was done to remove the probability of any residual protein adhering to the working electrode. The working electrode was stored in 0.1 M SPB (pH 7.0) at 4°C, when not in use. The working electrode was characterized by FTIR and SEM at several steps of its fabrication.

SEM and FTIR Spectroscopy of Working Electrode (POx/c-MWCNTs/CuNPs/PANI/AuE)

The SEM of bare AuE, PANI/AuE, c-MWCNTs/CuNPs/PANI/AuE, POx/c-MWCNTs/CuNPs/PANI/AuE were carried out on a commercial basis at Jawaharlal Nehru, New Delhi and FTIR of PANI/AuE, c-MWCNTs/CuNPs/PANI/AuE and POx/c-MWCNTs/CuNPs/PANI/AuE at Department of Biotechnology, University Institute of Engineering and Technology, Maharishi Dayanand University, Rohtak.

Construction & Testing of Pyruvate Biosensor Based on POx/c-MWCNTs/CuNPs/PANI/AuE

An improved amperometric pyruvate biosensor was fabricated, whereby POx/ c-MWCNTs/CuNPs/PANI/Au acted as a working electrode, silver/silver chloride as a reference electrode and Pt wire as supplementary electrode, were connected via a potentiostat/galvanostat. The potential was recorded by dipping the electrodes in a 25 ml, 0.1 M SPB (pH 7.0) consisting of 0.1 ml of 20 mM pyruvate.between a potential range of -0.1 V to 0.8 V.

Optimization of Pyruvate Biosensor Based on POx/c-MWCNTs/CuNPs/PANI/AuE

The biosensor conditions were analyzed and optimized in terms of pH by varying pH between 4.0 to 9.0 and preparing buffers of the specified pH range at an interval of 0.5. The temperature conditions were optimized between a range of 15- 50° C and pyruvate concentration in between 0.1 µM- 2000 µM.

Application of Pyruvate Biosensor (POx/c-MWCNTs/CuNPs/PANI/AuE)

Blood samples (2 ml each) were drawn from apparently healthy male, female and patients diagnosed with several heart ailments from local Pt. BDS Post Graduate Institute of Medical Science hospital and Holy Heart & Noble Heart, hospital. This collected blood samples were then centrifuged at 5000 rpm for 15 min, and the resulting supernatant (serum) was collected. The pyruvate level in the sera samples was enunciated by the present biosensor in the same way as illustrated for response measurement studies, under optimal working conditions except that pyruvate was replaced by serum sample. A standard curve was extrapolated between pyruvate concentrations versus current in µA, under standard assay conditions.

Evaluation of Pyruvate Biosensor (POx/c-MWCNTs/CuNPs/PANI/AuE)

The biosensor was evaluated in terms of the analytical performance by analyzing several parameters as described in (Malik *et al.*, 2019).

Stability of Working Electrode (POx/c-MWCNTs/CuNPs/PANI/AuE)

To test the shelf life of the working electrode, the activity of working electrode was recorded at regular intervals over duration of 8 months, when stored at 4° C.

Results and Discussion

Characterization of Copper Nanoparticles

The TEM images of the prepared copper nanoparticles revealed their tiny, round and spherical shape having a mean diameter of 19.70 nm and particle size lying between the range, 15.21 nm to 22.81 nm (Fig. 1a). The UV- visible spectra (Fig. 1b) of the nanoparticles displayed an explicitly high absorbance peak at 680 nm confirming the formation of copper nanoparticles. In addition to this, the characteristic peaks at 37.5, 43.5, 61.1 and 74.5 degrees analyzed via. XRD (Fig. 1c) were in direct correlation with the miller indices (literature values of face-cantered cubic), thereby inferring that the synthesized nanoparticles were pure and free of any kind of impurities since, no visible peaks that might arise due to impurities were observed in the XRD pattern.

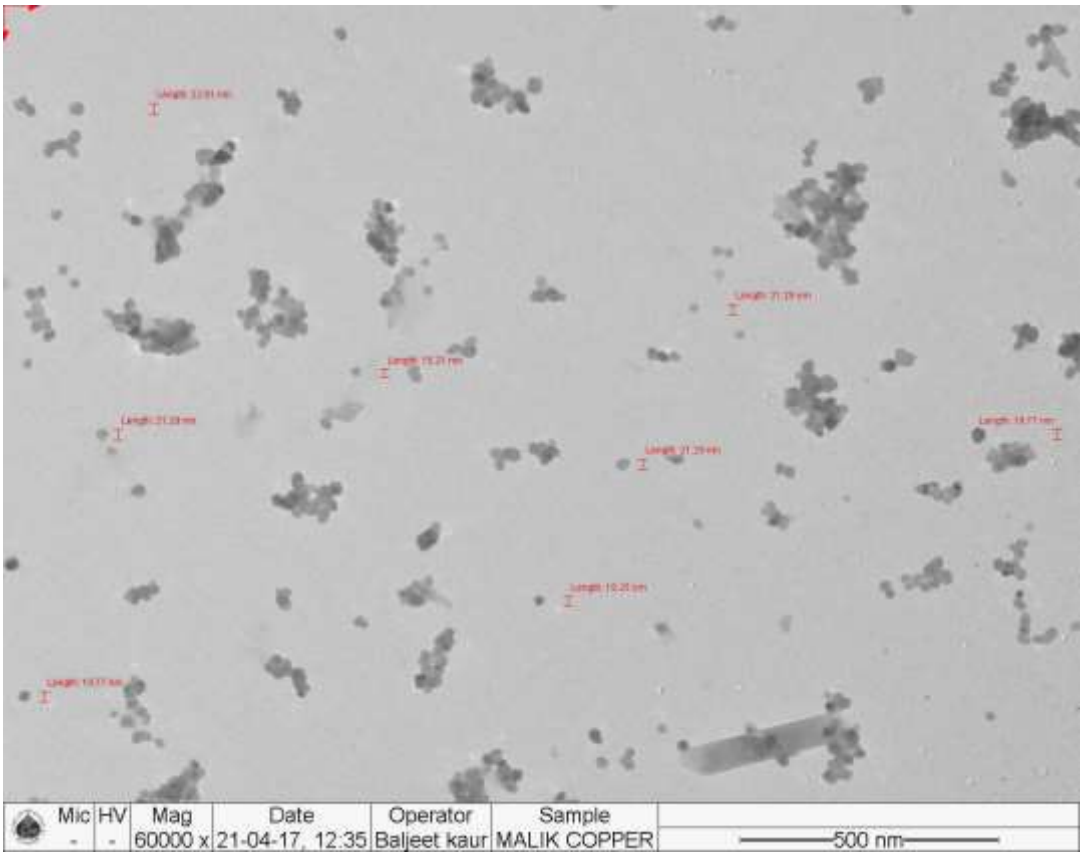

Fig. 1a: Characterization of copper nanoparticles (CuNPs) by transmission electron microscopy (TEM)

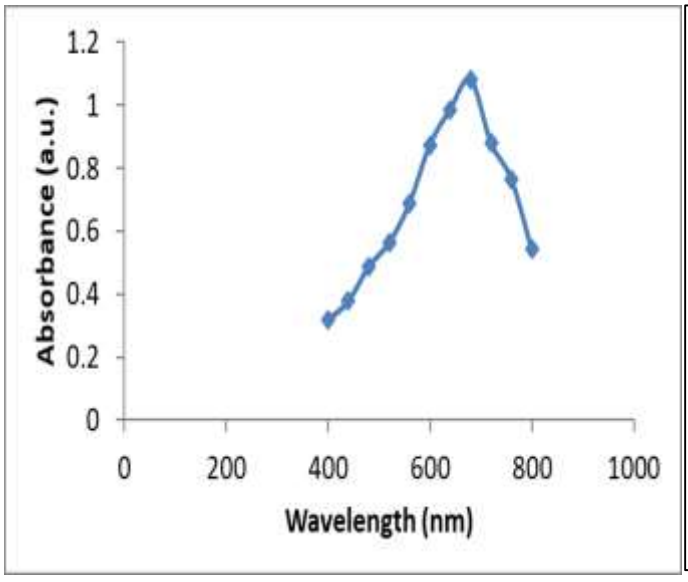

Fig. 1b: UV- Visible spectroscopy

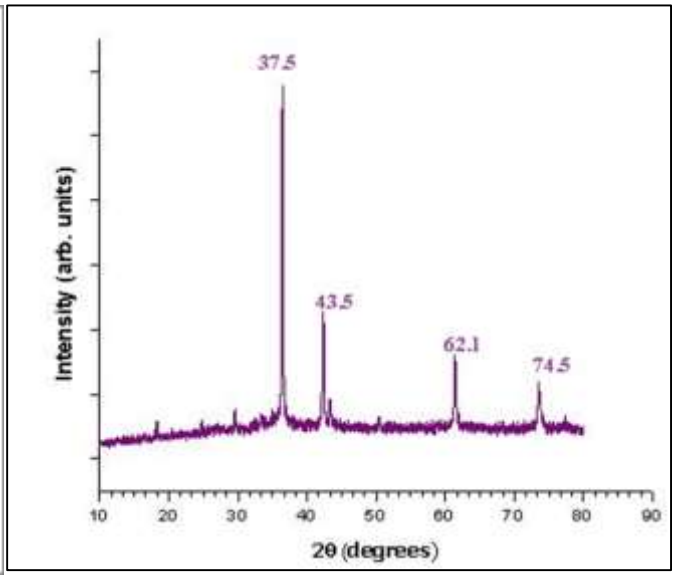

Fig. 1c: X- Ray Diffraction study

Characterization of Working Electrode (POx/c-MWCNTs/CuNPs/PANI/AuE) at Several Stages of Its Fabrication

By SEM

Fig. 2 displays a detailed microscopic view of the electrode during different stages of electro-deposition beginning with bare AuE, CuNPs/PANI/AuE, c-MWCNTs/CuNPs/PANI/AuE and finally, POx/c-MWCNTs/CuNPs/PANI/AuE respectively. A gradual modification in the structure of the bare gold electrode was clearly visible through these SEM images. And, it can be inferred that the deposition of these property enhancing nanomaterials was vehemently seen via. different SEM images. A uniform, smooth and featureless pictorial view was obtained by analyzing the bare electrode via SEM, which upon subsequent deposition with several nanomaterials resulted into the change in the morphology. The modified electrodes surface area was increased after deposition of these layers, which, further enhanced the flow of electrons and hence, resulted in an improved conductivity of the electrode as compared to the bare electrode. After immobilization of POx, the bulbous structure became visibly noticeable because of the interaction of the modified electrode with the POx.

By FTIR

The FTIR spectra (Fig. 3a) of copolymerized PANI/AuE showed peaks at 2991.46 cm-1 and 2355.36 cm-1, which can be attributed to the presence of NH stretching of benzenoid ring. The stretching vibrations at 3839.23 cm-1, 3740.00 cm-1 were due to the hydroxyl stretching vibration induced by the alcohol group. The peaks at 1509.07 cm-1 and 1129.18 cm-1 could be attributed to the quinonoid & benzenoid ring respectively. After electro deposition of the next two layers (Fig. 3b) of CuNPs and c- MWCNTs, a minor shift in the peak positions from 1509.07 cm-1 to 1503.11 cm-1 (aromatic C=C stretching) and 1129.18 to 1130.97 cm-1 (alkoxy C-O stretching) was observed. Other peaks at 2354.25 cm-1, 1698.72 cm-1depicted the presence of thiol SH moiety, C=O stretching attributed by the COOH groups present on the c- MWCNTs respectively. In addition, a peak at 1294.07 cm-1 might be possibly due to the interaction between the acyl C-O and phenol C-O groups. The immobilization caused by the enzyme (Fig. 3c) over the nanocomposite modified electrode revealed a deep and wider peak at 3220 cm-1 due to the presence of amine group in the enzyme. On the contrary, other peaks exhibited a renowned visible shift in the positions respectively i.e. from 1698. 72 cm-1 to 1579.82 cm-1, 1503.11 cm-1 to 1491.61 cm-1, 1294.07 cm-1 to 1303.39 cm-1 and finally a shift was visible from 1130.97 cm-1 to 1104.33 cm-1.

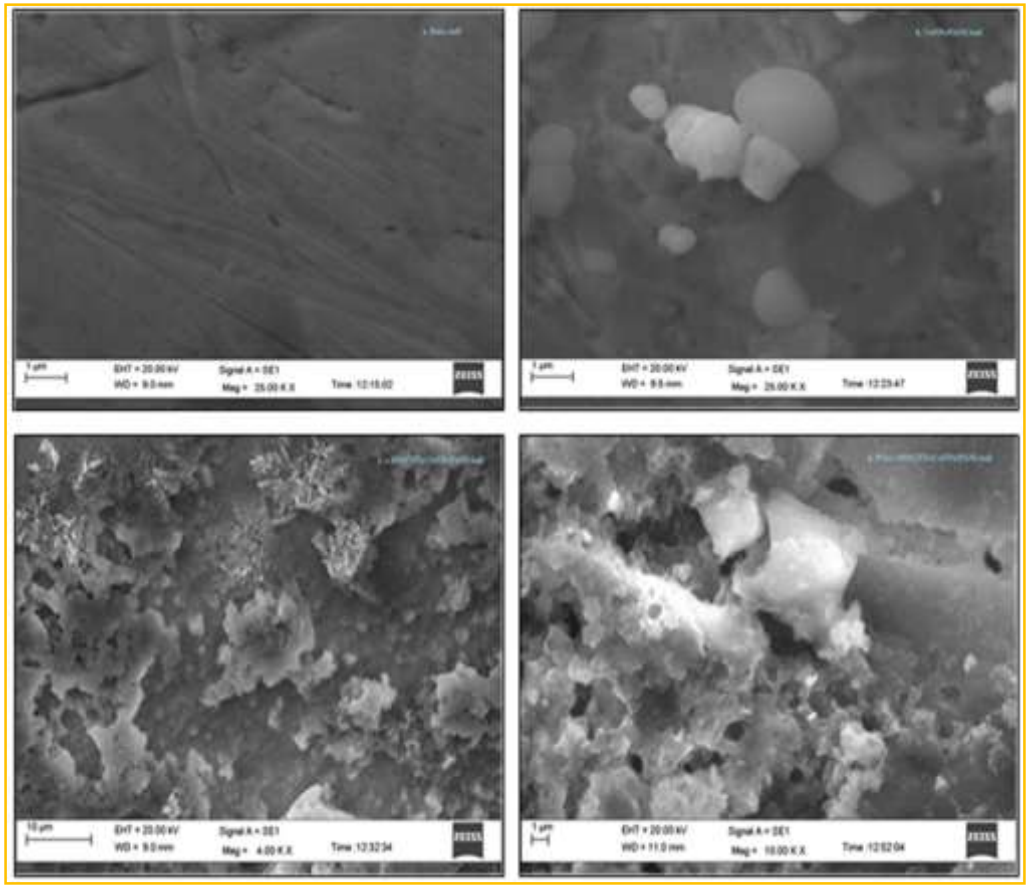

Fig. 2: Characterization of electrode by scanning electron microscopic images (SEM) at different stages of construction **(**a) Bare gold electrode (AuE); (b) PANI/CuNPs/AuE; (c) c-MWCNTs/CuNPs/PANI/AuE; (d) POx/c-MWCNTs/CuNPs/PANI/AuE

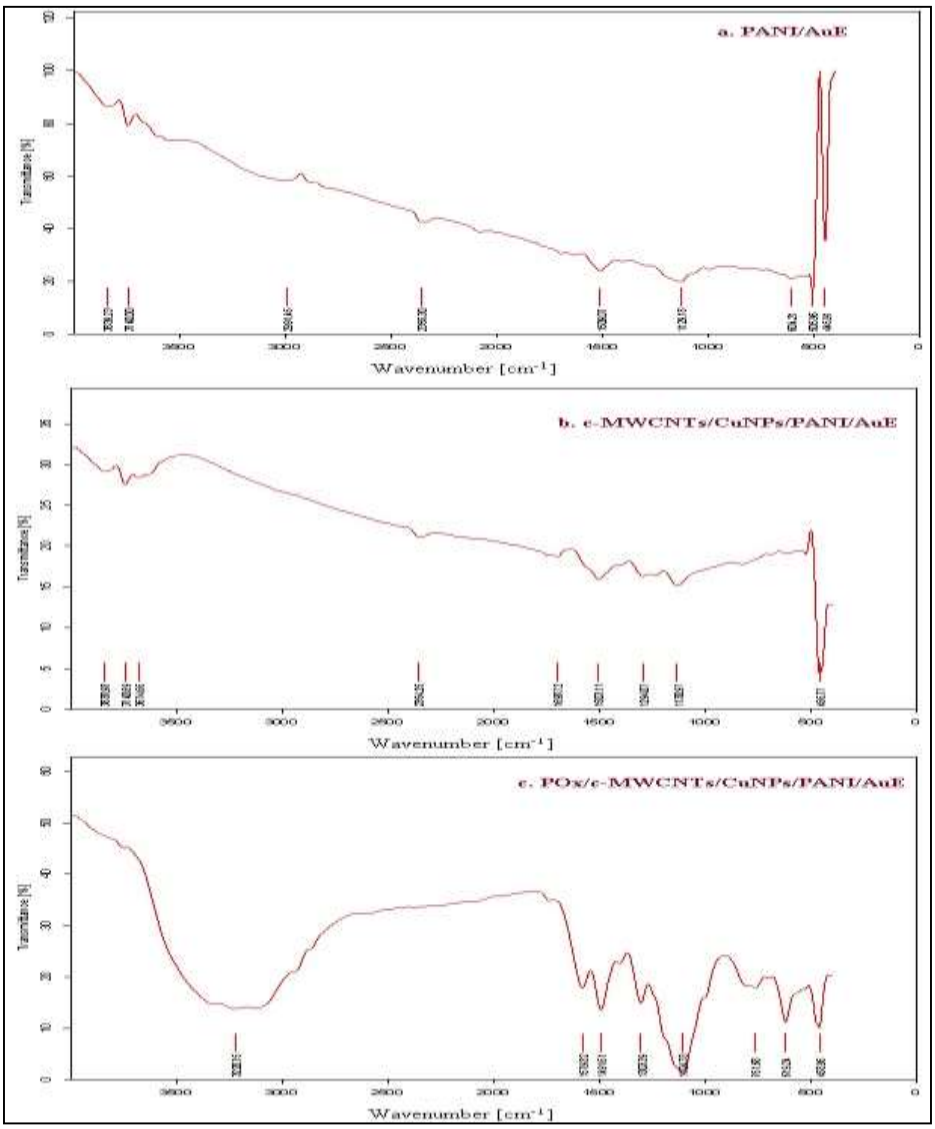

Fig. 3: Characterization of electrode by Fourier-transform infrared spectroscopy (FTIR) at different stages of construction (a) PANI/AuE; (b) c-MWCNTs/CuNPs/PANI/AuE; (c) POx/c-MWCNTs/CuNPs/PANI/AuE

Construction of Pyruvate Biosensor

A schematic illustration as shown in graphical abstract elucidates the fabrication of pyruvate biosensor whereby, covalent immobilization of POx on a nano-hybrid and uniform layer of PANI/CuNPs/c-MWCNTs electrodeposited onto the bare Au electrode was observed. The nanomaterials for co- polymerization i.e. PANI, CuNPs and c- MWCNTs were chosen since, the deposition of these materials is a facile method and the thickness of the layer could be managed easily. The modified electrode due to the presence of a heterogeneous layer of several nanomaterials shows enhanced electron transfer kinetics therefore, leading to improvement in the biosensor response and elevating the level of sensitive detection of the analyte of interest i.e. pyruvate, by the present biosensor. Next, immobilization of POx was made possible by the interaction between carboxyl and amine groups of EDC- NHS activated c- MWCNTs. EDC- NHS activated multi walled carbon nanotubes are known to possess - CHO and amine group to which the enzyme is found to couple and forms a strong covalent bond that lead to the development of a stable complex. The electrochemical reaction between POx and the substrate, pyruvate leads to the production of hydrogen peroxide, which on further breakdown upon application of high voltage leads to the production of electrons which was easily detected in the form of current. The level of current detected before and after immobilization was found to be elevated since, enzyme acts as a catalyst and enhances the signal strength and the rate of chemical reaction occurring within the electrochemical cell.

Cyclic voltammetric (CV) studies of pyruvate biosensor

The amperometric response (Fig. 4a) of c-MWCNTs/CuNPs/PANI modified AuE and POx/c-MWCNTs/CuNPs/PANI/AuE was recorded and the pattern of electrochemical behavior was analyzed by the present biosensor. The increase in the flow of current after deposition and immobilization demonstrated the uniform and enhanced response/ activity of the biosensor.

Response measurement of pyruvate biosensor

The present pyruvate biosensor exhibited a response time of 10 seconds at a potential of 0.5 V. This response measurement is based on fact that the biosensor showed maximum current response within an interval of 10 seconds. Thereby, inferring that it can detect the metabolite of interest (pyruvate) within 10 seconds.

Electrochemical impedance measurements

It was carried out to interrogate the impedance changes caused due to electro-deposition and immobilization of the nanomaterials and the enzyme respectively. Fig. 4b shows EIS of (a) bare AuE, (b) PANI/AuE (c) c-MWCNT/CuNPs/PANI/AuE (d) POx/c-MWCNT/CuNPs/PANI/AuE. The analysis for the impedance studies were carried out in a 5 mM miscible solution of potassium ferrocyanide/ potassium ferricyanide, respectively. The R_{CT} values are found to be directly correlated with the dielectric and insulating properties at the interface of electrode/electrolyte. The R_{CT} values for bare AuE, PANI/AuE, c-MWCNT/CuNPs/PANI/AuE and POx/c-MWCNT/CuNPs/PANI/AuE were recorded to be 2500 ohm, 2100 ohm, 400 ohm, 1750 ohm respectively. The decrease in the R_{CT} value was due to deposition of layers of nanomaterials resulting in elevated electron transfer efficiency. The immobilization of the enzyme molecules of POx lead to an increased efficacy as compared to the nanomaterial coated counterparts. These findings suggest that the enzyme was consistently immobilized over the electrode surface. In contrast, since biological molecules including, enzymes are poor conductors of electricity, they thereby are known to restraint electron transfer.

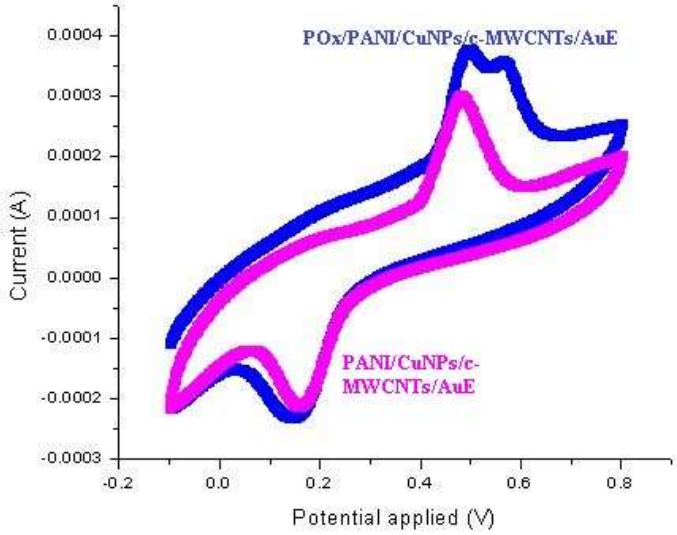

Fig. 4a: Response measurements studies of biosensor by cyclic voltammogram of c-MWCNTs/CuNPs/PANI/AuE and POx/c-MWCNTs/CuNPs/PANI/AuE (in 25 ml 0.1 M sodium phosphate buffer pH- 7.0 containing 0.1 ml of 20 mM pyruvate solution, 10 µl TPP and 10 µl FAD and 10 µl $MgCl_2$ under standard conditions at a scan rate of 20 mVs^{-1})

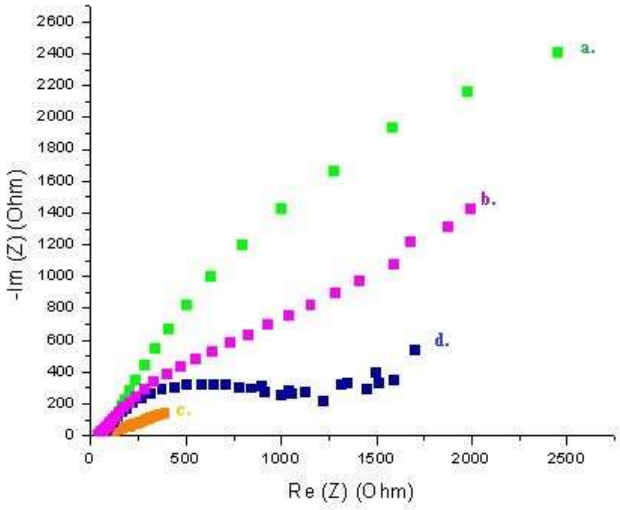

Fig. 4b: Electrochemical impedance spectra (EIS) of Bare AuE; PANI/AuE; c-MWCNTs/CuNPs/PANI/AuE; POx/c-MWCNTs/CuNPs/PANI/AuE

Optimization of Biosensor

The effects of several experimental parameters affecting the biosensor response were optimized such as the effect of pH, incubation temperature, time and substrate (pyruvate) concentration. The maximum current was obtained at a pH of 5.0 (Figure 5a), which is slightly lower than the pyruvate biosensor (pH- 5.7) explained in (Abayomi *et al.*, 2006), and higher than those biosensors described in (Abayomi *et al.*, 2006; Akyilmaz and Yorganci, 2008; Situmorang *et al.* 2002; Kulys *et al.*, 1992; Olsen, 1971; Bayram and Akyilmaz, 2014). This optimum pH of the modified electrode showed variation from the pH of the native enzyme due to the amalgamation of several functional groups present in the active center of the electrodeposited nanomaterials and the enzyme. Figure 5b displayed the optimum temperature at 35°C, beyond this, the response of the biosensor declined due to the thermal denaturation of the enzyme. As compared to the earlier cited biosensors, this optimum temperature of 35°C (Figure 4b) was found to be similar to the biosensor cited in (Akyilmaz and Yorganci, 2008) and near to the biosensor (30°C) described in (Berntsson, 1955). The experimental efficiency of the working electrode at 35°C could avoid the process of loss of activity of the enzyme due to the process of denaturation of enzyme and thus, helped enhance the shelf life of enzyme electrode.

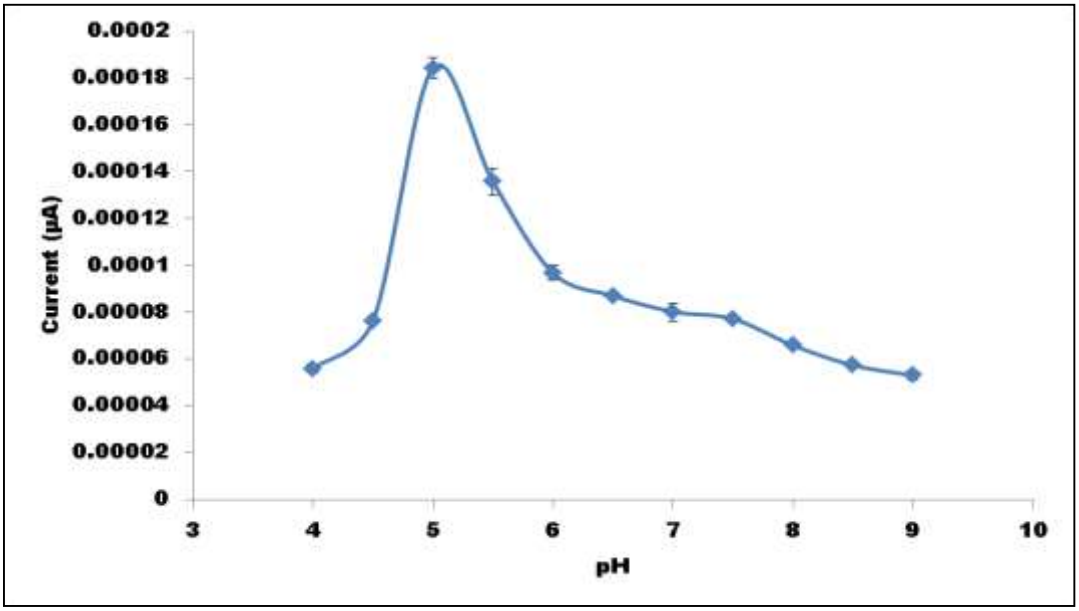

Fig. 5a: Influence of pH on the current response

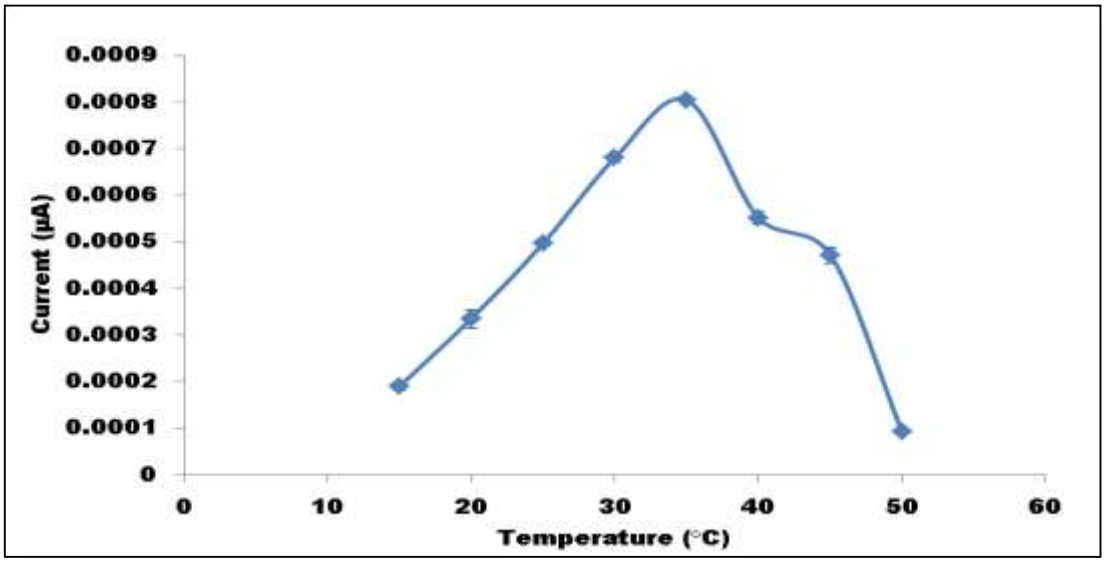

Fig. 5b: Effect of incubation temperature

Evaluation of Biosensor

The fabricated biosensor exhibited a linear response between pyruvate concentration of 0.1- 2000 µM, under standard assay conditions (Fig.5c). This observation is found to be one step ahead than the previously elucidated biosensors (Li *et al*., 2017; Ghica and Brett, 2006; Gajovic *et al.*, 2000; Rezvin *et al.*, 2002) and, almost similar to 0 µM-2000 µM cited by Rezvin *et al.* 2002. However, this range was lower than the wide concentration range of pyruvate biosensor based on enzyme nanoparticles of POx (Malik *et al.*, 2019). The LOD was calculated to be 0.72 µM, which is far better than most of the earlier described biosensors available till date (Akyilmaz and Yorganci, 2008, Li *et al.*, 2017; Berntsson, 1955; Gajovic *et al.*, 2006; Maines *et al.*, 2000; Knyzhnykova *et al.*, 2018; Mizutani *et al.*, 1980). This LOD was not lower than that of pyruvate biosensor based on POxNPs/AuE (Malik *et al.*, 2019). The analytical recoveries of added pyruvate in sera at levels of 1.0 mM and 2.0 mM were 99.6% and 99.2% respectively, signifying the reliable fabrication of the present biosensor. The determination of the pyruvate by the present nanocomposite modified gold electrode was carried out in serum samples back to back five times on day one (within batch) and after storing the same samples for one week at -20°C (between batch). The CV in serum pyruvate was 0.069% and 0.072% respectively. These extremely specific values express that the present biosensor is a competent and reliable model exhibiting virtuous reproducibility.

Applications of Pyruvate Biosensor

The present biosensor revealed sera pyruvate level of healthy adults in between 57.5 µM±1.85 to 113.4 µM±1.02, which confers normal range as found in the blood. Whilst, the diseased patients experiencing cardiogenic stress showed pyruvate values to be in the range, 150.4 µM±3.27 to 408.1 µM±1.06, which is significantly elevated than the healthy individuals (Table 1).

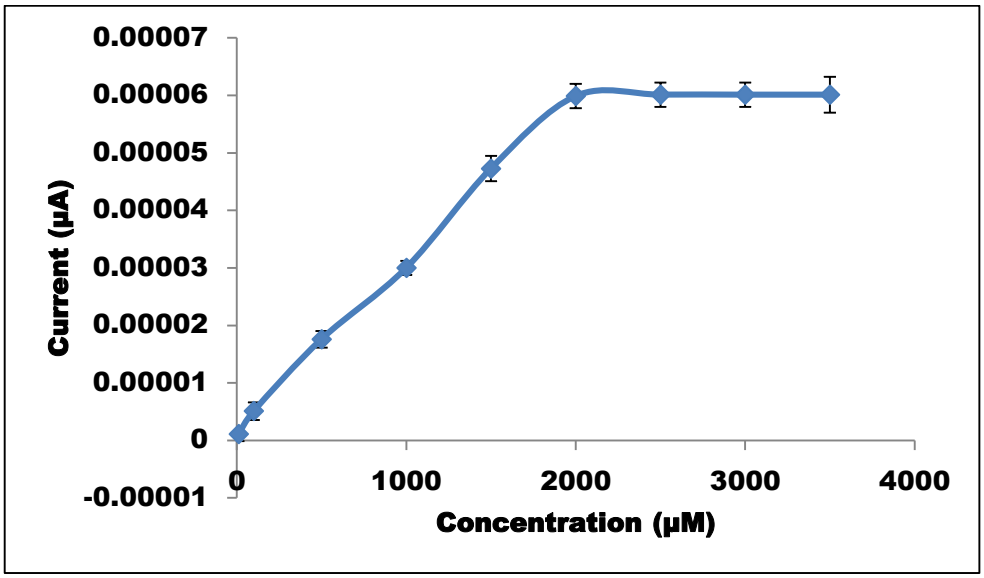

Fig. 5c: Effect of pyruvate concentration on nanocomposite modified enzyme electrode

Table: 1 Serum pyruvate levels of apparently healthy adults and persons suffering from cardiogenic stress, as measured by pyruvate biosensor based on POx/c-MWCNTs/CuNPs/PANI/AuE

Age group (years)	Sex	n	Pyruvate value (µM)(mean± SD)	
			Healthy individuals	Diseased individuals
30-40	Male	5	68.0±1.02	335.2±1.41
	Female	5	57.5±1.85	150.4±3.27
40-50	Male	5	74.2±2.20	263.4±1.01
	Female	5	84.2±1.37	168.6±1.62
50-60	Male	5	90.8±1.32	154.2±2.03
	Female	5	71.6±1.87	169.7±2.07
60-70	Male	5	57.8±2.54	187.3±1.18
	Female	5	79.8±3.01	176.1±1.31
70-80	Male	5	90.4±3.34	408.1±1.06
	Female	5	87.2±1.87	210.7 ±2.03
80-90	Male	5	110.5±2.04	289.1±1.21
	Female	5	113.4±1.02	215.8±2.12

(POx- Pyruvate oxidase; c-MWCNTs- Carboxylated multi-walled carbon nanotubes; CuNPs- Copper nanoparticles; PANI- Polyaniline; AuE- Gold electrode)

Correlation Coefficient Analysis

A correlation curve was plotted by recording the sera pyruvate values of healthy adults and diseased patients by present biosensor and the reference spectrophotometric method (Berntsson, 1955). On analyzing, an excellent correlation coefficient (R2= 0.9974) with regression equation being y= 2E-06x was achieved between the values by these two methods, (Fig. 6). These interpretations conveyed extreme accuracy of the present biosensor.

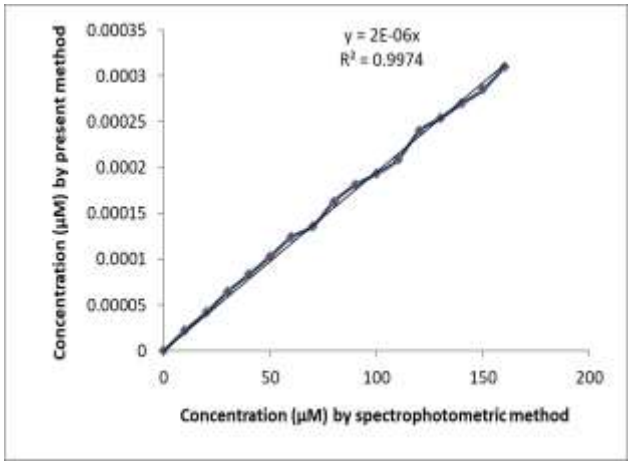

Fig. 6: Correlation curve between sera pyruvate values as measured by standard colorimetric (X- axis) method and the present biosensor (Y- axis) based on POx/c-MWCNTs/CuNPs/PANI/AuE.

Selectivity and Anti- Interference Ability

The interference of various components was examined to conclude the selectivity and specificity of the present biosensor. POx/c-MWCNTs/CuNPs/PANI/AuE revealed superb anti- interference capability with numerous chief blood components such as urea, uric acid, ascorbic acid, glucose and lactic acid at their physiological concentrations. Uric acid and lactic acid did not interfere with the biosensor response, fact attributable to the employment of low potential of 0.5 V during experimental proceedings. While, some blood components like urea, ascorbic acid, glucose displayed interference by only 6.78%, 9.54% and 6.84% respectively. Thereby, it can be concluded that the biosensor exhibited only minor interference (0-10%) in its working in presence of all potential interfering metabolites. Precise selectivity of pyruvate was observed on the biosensor current response, conferring that it is highly sensitive for the determination of pyruvate.

Long Term Stability of the Modified Electrode

The shelf life of the fabricated electrode was analyzed by recording the change in response after every 30 days, while being stored at 4°C. The reusability of the present biosensor was high as compared to the ones cited in the literature and exhibited storage stability for over 200 days (Fig. 7). The working electrode deterred by only 20% in its working after continual usage for duration of 8 months. The working electrode was known to have higher reusability than 14 days (Maines *et al*., 2000); (Ghica and Brett, 2006), 90 days (Situmorang *et al.,* 2002), >60 days (Kulys *et al.*, 1992), >10 days (Li *et al.*, 2017), 5 hours (Mizutani *et al*., 1980); 7 days (Mizutani *et al.*, 2000), but comparable to enzyme nanoparticles based pyruvate biosensor (240 days)(Malik *et al.*, 2019).

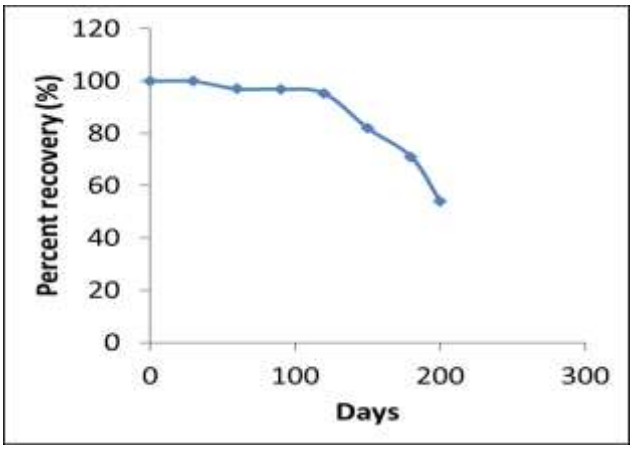

Fig. 7: Storage stability of POx/c-MWCNTs/CuNPs/PANI/Au electrode in 0.1 M sodium acetate buffer (pH- 5.0) at 4ºC.

Comparison of pyruvate biosensors based on enzyme bound to nanocomposite and enzyme nanoparticles (ENPs)

A comparison of construction, optimization and analytic properties of both the pyruvate biosensors based on enzyme (POx) bound to nanocomposite (cMWCNTs/CuNPs/PANI) electrodeposited onto Au electrode and enzyme nanoparticles (POxNPs) directly bound to Au electrode is summarized in Table 2, which suggest that enzyme nanoparticles (ENPs) based pyruvate biosensor is better than that based on enzyme bound to nanocomposite in terms of construction, analytic performance and shelf life.

Conclusion

The pyruvate bionanosensor based on enzyme bound to nanocomposite (POx/c-MWCNTs/CuNPs/PANI/AuE) exhibited very quick response time (10 seconds), with a low LOD (0.72 µM), wider linear working range (0.1 to 2000 µM), good reproducibility and an enhanced shelf life (200 days). All these parameters helped to improve the analytical and detection precision of the biosensor, which was mainly due to the deposition of hybrid layer of the nanocomposites (c-MWCNTs/CuNPs/PANI). However, a comparison of enzyme nanoparticles (ENPs) based pyruvate biosensor with the present biosensor based on enzyme bound to nanocomposite has revealed the superiority of ENPs based biosensor over nanocomposite based biosensor in terms of construction, analytic performance and shelf life. Hence, research in the coming years could be focused on ENPs based biosensors for detection of other metabolites.

Table 2: A comparison of analytical parameters of amperometric pyruvate biosensors based on covalent immobilization of native enzyme onto nanohybrid electrodeposited onto Au electrode (POx/cMWCNT/CuNPs/PANI/AuE) and enzyme nanoparticles directly onto Au electrode (POxNPs/AuE)

S. N.	**Construction/Analytical parameters**	**Pyruvate biosensor based on enzyme bound to nanohybrid (POx/c-MWCNTs/CuNPs/PANI/AuE)**	**Pyruvate biosensor based on enzyme nanoparticles bound to Au electrode (POxNPs/AuE)**
1.	Method of construction	Complicated	Simple
2.	Cost of construction	High	Low
3.	Immobilization of enzyme onto electrode	Indirect (Through EDC-NHS chemistry)	Direct
4.	Linearity/working range(µM)	0.1-2000	0.01-5000
5.	Detection limit (µM)	0.72	0.67
6.	Analytical recovery (%)	99.2	99.5
7.	Precision: Within and between batch CV (%)	0.069 and 0.072	0.045 and 0.040
8.	Correlation with standard spectrophotometric i.e. R^2 value	0.9974	0.999
9.	Interference by metabolites (at physiological conc.)	< 10%	< 10%
10.	Storage stability (dry at 4°C)(days)	200	240

Acknowledgements

The authors are highly thankful to the Directors of all the Hospitals mentioned in the study for providing with the sera samples of apparently healthy persons and cardiogenic patients.

Conflict of Interest

The authors have no conflict of interest.

References

Abdolahi A, Hamzah E, Ibrahim Z and Hashim S (2012) Synthesis of uniform polyaniline nanofibers through interfacial polymerization. *Materials* (Basel) **5:** 1487–1494. DOI: 10.3390/ma5081487

Abayomi LA, Terry LA, White SF and Warner PJ (2006) Development of a disposable pyruvate biosensor to determine pungency in onions (Allium cepa L.). *Biosens Bioelectron.* **21:** 2176–2179. DOI: 10.1016/j.bios.2005.10.024

Akyilmaz E and Yorganci E (2008) A novel biosensor based on activation effect of thiamine on the activity of pyruvate oxidase *Biosens Bioelectron* **23:** 1874–1877. DOI: 10.1016/j.bios.2008.03.001

Anthon GE and Barrett DM (2000) Modified method for the determination of pyruvic acid with dinitrophenylhydrazine in the assessment of onion pungency. *J. Sci. Food Agric.* **83. DOI:** 10.1002/jsfa.1525

Berntsson S (1955) Spectrophotometric Determination of Pyruvic Acid by the Salicylaldehyde Method. *Anal Chem* **27:** 1659–1660. DOI: 10.1021/ac60106a051

Bayram E and Akyilmaz E (2014) A new pyruvate oxidase biosensor based on 3-mercaptopropionic acid/6-aminocaproic acid modified gold electrode. *Artif Cells Nanomedicine Biotechnol* **42:** 418–422. DOI: 10.3109/21691401.2013.815626

Dagar K and Pundir CS (2017) An improved amperometric L-lactate biosensor based on covalent immobilization of microbial lactate oxidase onto carboxylated multiwalled carbon nanotubes/copper nanoparticles/polyaniline modified pencil graphite electrode, *Enzyme Microb Technol* 96. DOI: 10.1016/j.enzmictec.2016.10.014

Din MI and Rehan R (2017) Synthesis, Characterization, and Applications of Copper Nanoparticles. *Anal Lett* **50:** 50–62. DOI: 10.1080/00032719.2016.1172081

Essa MM, Subash S, Braidy N and Al-Adawi, S, Lim CK, Manivasagam T and Guillemin GJ (2013) Role of NAD+, oxidative stress, and tryptophan metabolism in autism spectrum disorders. *Int J Tryptophan Res* **6:** 15–28. DOI: 10.4137/IJTR.S11355

Gray LR, Tompkins SC and Taylor EB (2014) Regulation of pyruvate metabolism and human disease. *Cell Mol Life Sci* **71:** 2577–2604. DOI: 10.1007/s00018-013-1539-2

Ghica ME and Brett CMA (2006) Development of novel glucose

and pyruvate biosensors at poly(neutral red) modified carbon film electrodes. Application to natural samples. *Electroanalysis* **18:** 748–756. DOI: 10.1002/elan.200503468

Gajovic N, Binyamin G, Warsinke A, Scheller FW and Heller A (2000) Operation of a miniature redox hydrogel-based pyruvate sensor in undiluted deoxygenated calf serum. *Anal Chem* **72:** 2963–2968. DOI: 10.1021/ac991021i

Jariwala D, Sangwan VK, Lauhon LJ, Marks TJ and Hersam MC (2013) Carbon nanomaterials for electronics, optoelectronics, photovoltaics, and sensing. *Chem Soc Rev* 42 (2013) 2824–2860. DOI: 10.1039/c2cs35335k

Kulys J, Wang L and Daugvilaite N (1992) Amperometric methylene green-mediated pyruvate electrode based on pyruvate oxidase entrapped in carbon paste. *Anal Chim Acta* **265:** 15–20. DOI: 10.1016/0003-2670(92)85149-Z

Knyzhnykova DV, Topolnikova YV, Kucherenko IS and Soldatkin OO (2018) Development of pyruvate oxidase-based amperometric biosensor for pyruvate determination. *Biopolym Cell* **34:** (2018) 14–23. DOI: 10.7124/bc.00096C

Li YS, Li QJ, Yang W and Gao XE (2017) Research on a new micro volume fluorescence capillary biosensor assay for sequentially quantifying pyruvate and lactate. *J Fluoresc* **27:** 883-894. DOI: 10.1007/s10895-017-2024-3

Malik M, Chaudhary R and Pundir CS (2019) An improved enzyme nanoparticles based amperometric pyruvate biosensor for detection of pyruvate in serum, *Enz Microbial Technol* **123:** 30-38. DOI: 10.1016/j.enzictec.2019.01.006

Mizutani F, Tsuda K, Shuichi IK and Matsumoto SK (1980) Determination of glutamate pyruvate transaminase and pyruvate with an amperometric pyruvate oxidase sensor *Anal Chim Acta* **118:** 65–71. DOI: 10.1016/S0003-2670(01)93714-6

Mizutani F, Yabuki S, Sato Y, Sawaguchi T and Ijima S (2000) Amperometric determination of pyruvate,phosphate and urea using enzyme electrodes on pyruvate oxidase - containing (poly alcohol)/polyion complex- bilayer membrane. *Electro Chim Acta* **45:** 2945-2952. DOI: 10.1016/S0013-4686(00)00373-X

Maines A, Prodromidis MI, Tzouwara-karayanni SM, Karayannis MI and Ashworth D (2000) An Enzyme Electrode for Extended Linearity Citrate Measurements Based on Modified Polymeric Membranes. *Electroanalysis* 1118–1123. DOI: 10.1002/1521-4109(200010)12:14<1118::AID-ELAN1118>3.0.CO;2-0

Olsen C (1971) An enzymatic fluorimetric micromethod for the determination of acetoacetate, β-Hydroxybutyrate, pyruvate and lactate. *Clin Chim Acta* **33:** 293–300. DOI: 10.1016/0009-8981(71)90486-4

Pundir CS, Malik M and Chaudhary R (2019) Quantificatuion of pyruvate with special emphasis on biosensors:A review. *Microchem J* **146:** 1102- 1112 DOI: 10.1016/j.micro.2019.02.046

Revzin AF, Sirkar K, Simonian A and Pishko MV Glucose, lactate, and pyruvate biosensor arrays based on redox polymer/oxidoreductase nanocomposite thin-films deposited on photolithographically patterned gold microelectrodes. *Sensors Actuators B Chem* **81:**359–368. DOI: 10.1016/S0925-4005(01)00982-0

Situmorang M, Gooding JJ, Hibbert DB and Barnett D (2002) The development of a pyruvate biosensor using electrodeposited polytyramine. *Electroanalysis* **2:** 17–21. DOI: 10.1002/1521-4109(200201)14:1<17::AID-ELAN17>3.0.CO;2-O

Shapiro F and Silanikove N (2011) Rapid and accurate determination of malate, citrate, pyruvate and oxaloacetate by enzymatic reactions coupled to formation of a fluorochromophore: Application in colorful juices and fermentable food (yogurt, wine) analysis. *Food Chem* **129:** (2011) 608–613. DOI: 10.1016/j.foodchem.2011.04.074

Yoo KS and Pike LM (1999) Development of an automated system for pyruvic acid analysis in onion breeding. *Sci Hortic* (Amsterdam) **82:** 193–201. DOI: 10.1016/S0304-4238(99)00075-8

Zapta-Bacri AM and Burstein C (1987) Enzyme elecrtode composed of the pyruvate oxidase from Pediococcus species coupled to an oxygen electrode for measurement of pyruvate in biological media. *Biosensors* **3**(4): 227-237. DOI: 10.1016/0265-928X(87)85003-4